

Technical Note

Optimisation of sensor positions in random linear arrays based on statistical relations between geometry and performance

Lara del-Val*, María Jiménez, Alberto Izquierdo, Juan Villacorta

Departamento de Teoría de la Señal y Comunicaciones e Ingeniería Telemática, University of Valladolid, Spain

ARTICLE INFO

Article history:

Received 5 October 2010

Received in revised form 6 July 2011

Accepted 6 July 2011

Available online 31 July 2011

Keywords:

Array design

Acoustic array

Sidelobe level performance

ABSTRACT

Due to the widespread use of acoustic arrays, optimisation techniques for array design, focused on improving array performance, have been widely published. This paper exploits the statistical relation between different measures of sidelobe levels and the spacing of elements in random linear arrays made up of a small number of sensors. This paper defines the methodology to obtain maximum probability functions, associating array geometry and performance. These maximum probability functions allow a pre-selection of those array geometries that are more likely to be associated to specified sidelobe level values. This pre-selection results in a significantly reduced computational burden.

© 2011 Elsevier Ltd. All rights reserved.

1. Introduction

There are many solutions based on the use of acoustic arrays, mostly microphone arrays, such as the analysis of wheel/rail noise radiation [1], localization of acoustic sources [2], analysis of diffuse fields [3], or sound source imaging of flying targets [4]. With the spread of sensor arrays, many studies on pattern synthesis techniques were developed in order to improve array performance. First, these techniques were based on the variation of sensor excitations (amplitude and phase) [5], keeping sensors uniformly distributed. Then, techniques based on varying sensor positions, with uniform sensor excitations, were developed [6,7], and after that, algorithms that optimise simultaneously sensor excitations and positions [8] came up.

Sidelobe levels can be reduced by varying sensor positions, either following certain rules [6] (aperiodic arrays) or in a random manner [7], in this case, mainbeam width can increase [9], it must be handled with care. Random arrays offer more control over the array beam pattern than aperiodic ones [7]. The study shown in this paper is based on varying randomly only sensor positions to improve array performance, so the amplitudes of sensor excitations have been kept constant and equal to 1.

Over the years, several methods for array geometry design have been developed. It is clear that there is a relationship between sensor positions, i.e. array geometry, and array sidelobes performance [7]. Establishing such a relationship in a statistical sense is the starting point of this work; and once these relationships are

defined, the next step is to analyse them to find their potential applications on pattern synthesis techniques.

Despite the multiple theoretical studies of random arrays, such as those carried out by Lo [10], these studies are centred in large arrays. These works show techniques that converge when applied to arrays with a large number of sensors. They are not valid for small arrays. Thus, the analysis shown in this paper is centred in arrays with a reduced number of elements. This paper defines relationships between some array geometric features, based on the array sensor spacing, and the array performance, based on its sidelobe levels. Employing these relations on array design techniques can reduce the computational burden related to the array design process. These relationships can be used to pre-select only those arrays whose geometry is suitable to reach the expected performance.

2. Array characterization

In this analysis, random linear arrays with omnidirectional sensors whose positions follow a uniform random distribution have been selected. A fixed spatial aperture was used in this analysis, in order to fix the mainbeam width. This width depends mainly on the overall array length [10], called spatial aperture. Thus, avoiding mainlobe widening allows the analysis of array performance only on the basis of its sidelobe level values. Spatial aperture of a classic Uniform Linear Array (ULA) with $\lambda/2$ sensor spacing has been taken as reference for all random arrays. The spatial aperture of a ULA is defined as: $A_p = (N - 1) * X_i$, being N the number of array sensors and X_i the sensor spacing, which, in this case, is constant and equal to $\lambda/2$.

* Corresponding author.

E-mail address: lara.val@tel.uva.es (L. del-Val).

Maximum sensor spacing is limited by this spatial aperture constraint, while minimum spacing is limited by the physical dimensions of the array elements. Mutual coupling is avoided by forcing minimum spacing to be greater than $\lambda/4$.

2.1. Sidelobe parameters

Most representative sidelobe levels have been chosen for this analysis:

- First sidelobe level (SLL_1): It is the largest level of the pair of sidelobes that are closer to the mainlobe, on the right and on the left.
- Maximum sidelobe level (SLL_{max}): It is the level of the largest sidelobe that is shown in the beampattern. This sidelobe parameter includes the grating lobe concept [9].
- Average sidelobe level (\overline{SLL}): It is the average of all levels of the sidelobes in the beampattern.

All of them are expressed in decibels, and all of them are relative to the level of the main beam.

2.2. Array geometric features

The array geometric parameters selected for this study are based on a linear array of N sensors with X_i spacing between consecutive sensors ($X = [X_1 X_2 \dots X_{N-1}]$). Specifically for this research, the following geometric features have been chosen

- Spacing standard deviation

$$\sigma_X = \sqrt{\left[1/(N-1)\right] \cdot \sum_{i=1}^{(N-1)} (X_i - \bar{X})^2} \quad (1)$$

where \bar{X} is the spacing mean:

$$\bar{X} = \left[1/(N-1)\right] \cdot \sum_{i=1}^{N-1} X_i \quad (2)$$

- Maximum spacing

$$X_{max} = \max_{N-1} (X_i) \quad (3)$$

Previous studies [11] showed that minimum sensor spacing is not an appropriate parameter to be related to the array sidelobe levels.

These geometric features have been calculated for each array in order to find the relationship of each one to each sidelobe parameter, getting six different relation pairs.

3. Method

Once the parameters of the analysis are specified, the next procedure is:

- M random linear arrays A_m ($0 \leq m \leq M-1$) are created, fulfilling the defined spatial aperture and sensor minimum spacing constraints.
- S and G are defined as the variables that are associated to sidelobe levels and geometric features, respectively.
- The (S,G) set of values is quantified, being Δs and Δg the sidelobe level and geometric feature quantification intervals, respectively. The indexes associated to a (S,G) pair of values are defined as: $i = E[S/\Delta s]$ and $j = E[G/\Delta g]$, being $E[\cdot]$ the integer part function.

- A discrete two-dimensional histogram, $F(i,j)$, is defined. This histogram represents the number of random arrays whose (S,G) pair of values is in each interval: $F(i,j) = \text{count}_{0 \leq m \leq M-1} (A_m \mid i \cdot \Delta s \leq S_m \leq (i+1) \Delta s, j \cdot \Delta g \leq G_m \leq (j+1) \Delta g)$.

Fig. 1 shows, as an example, one of the six 2D histograms defined for the analysis of random linear arrays with $N = 8$ and $A_p = 7\lambda/2$. It is represented using contour lines in such a way that darker lines show higher values of the histogram, representing a higher density of arrays, and lighter lines show lower values, representing a lower density of arrays.

In this histogram, it can be observed that, although array sensor positions follow a uniform random distribution, the distribution of the frequency of occurrence is not uniform. This fact is shown in the histogram by means of a non uniform density of arrays. In the histogram, there are areas formed by cells with a high number of arrays, where there is a high probability to find random arrays with a given geometric and sidelobe level pair of values. It can also be observed that there are also areas with cells with a null value, meaning that it is very unlikely, or even impossible, to obtain arrays with specific geometric and sidelobe level pairs of values. This histogram also shows that as the array performance improves, i.e. sidelobe level values decrease, the frequency of occurrence decreases, so the number of possible arrays that offer good performance values decreases.

To extract the meaningful information of these 2D histograms, one geometric value is associated to each discrete sidelobe level value, according to the following methodology:

- Each $i \cdot \Delta s$ is associated to a $j \cdot \Delta g$ value so that, for each i value, $F(i,j)$ is maximized.
- A continuous one-dimensional function is defined interpolating the associated $j \cdot \Delta g$ values on a least square sense. These functions are called “maximum probability functions”. An example represented with a black striped line in the histogram is shown in Fig. 1.

In this way, the two-dimensional information of the histograms is reduced to linear functions which allow, on the basis of maximum probability values, an easy, direct and effective procedure for array selection.

As an example, the left image of Fig. 2 shows the three maximum probability functions that relate X_{max} to each of the three sidelobe levels of the analysis for random linear arrays with $N = 8$ and $A_p = 7\lambda/2$.

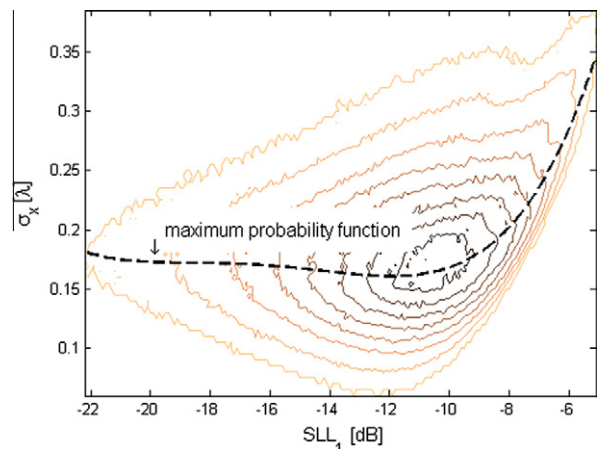


Fig. 1. 2D histogram.

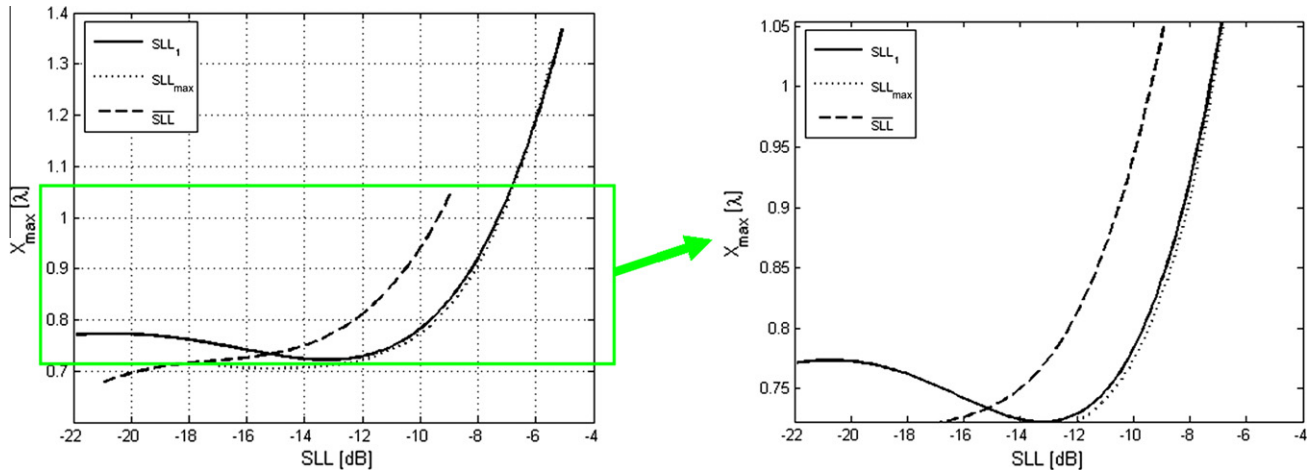


Fig. 2. Maximum probability functions. Effective area definition. *SLL* interrelationship procedure.

4. Analysis of the relationships

Three maximum probability functions are shown in the same figure, associating the three defined sidelobe level parameters with the same geometric feature. Thus, studying the geometrical features of a set of arrays, a pre-selection of those with a certain sidelobe level performance can be carried out. Also, from a pre-defined sidelobe level, a set of constraints on the geometry of the array can be established.

The following information can also be inferred from these figures:

4.1. Most probable limits of sidelobe level values

Most probable limits of sidelobe level values for random linear arrays formed by N sensors and with a $(N - 1)\lambda/2$ spatial aperture can be extracted from these curves. As an example, the specific limits for random arrays with $N = 8$ and $A_p = 7\lambda/2$ are shown in Table 1.

These minimum limits are very interesting in array design, since an improvement on array performance is equivalent to a reduction of its sidelobe levels. On the other hand, maximum limits show the most probable worst behaviours of sidelobes that could be found working with random linear arrays with certain number of sensors and spatial aperture.

Looking at Table 1, it can be observed that SLL_1 and SLL_{\max} minimum limits, for random linear arrays with $N = 8$ and $A_p = 7\lambda/2$ (-22 dB and -17 dB, respectively), are different; probably because the highest sidelobe is not usually the first one in random arrays with a defined spatial aperture and minimum spacing constraints.

4.2. Sidelobe level interrelationship

In order to establish relationships between parameters, an “effective” working area has been defined on the y -axis (geometric parameter) for each set of functions. In this “effective area”, a given value of the geometric parameter is related to a certain value of each sidelobe level of the study. The effective area covers from the lowest of the highest geometric values related to each of the three sidelobe levels to the highest of the corresponding three lowest geometric values. An example of the definition of one of these effective areas is shown in Fig. 2.

Once the effective area is defined, the next step is to create a procedure to interconnect these three sidelobe levels, from a

Table 1

Most probable limits of sidelobe level values.

	Maximum (dB)	Minimum (dB)
SLL_1	-5	-22
SLL_{\max}	-5.3	-17
\overline{SLL}	-7	-21

specific value of one of the defined geometric parameters. This procedure has the following steps:

- A value for any of the three sidelobe levels is specified.
- From this value, its corresponding maximum probability value of the geometric feature is obtained.
- Then, from this geometric feature value, maximum probability values of the remaining two sidelobe levels are acquired.

An example of this procedure, relating *SLL* values through the corresponding X_{\max} value for random linear arrays of eight sensors with a $7\lambda/2$ spatial aperture, is shown in the right image of Fig. 2:

- First, a first sidelobe level (SLL_1) value is specified. In this example, $SLL_1 = -18$ dB.
- From the function that connects sidelobe level (SLL_1) to the geometric feature (i.e. X_{\max}), i.e. the solid curve, the X_{\max} value that corresponds to the fixed SLL_1 value is acquired. In this example, $X_{\max} = 0.763\lambda$.
- Once this most probable value of the geometric feature is specified, it is necessary to obtain the maximum probability values of the two remaining sidelobe levels (SLL_{\max} and \overline{SLL}) related to the acquired value of the geometric feature. In the example, $X_{\max} = 0.763\lambda$ corresponds to a value $SLL_{\max} = -10.3$ dB - the dashed curve - and to a value $\overline{SLL} = -13.5$ dB - the dash dotted curve.

This procedure establishes an interrelationship between these three sidelobe levels. These functions show a way to connect most probable values of sidelobe levels through an array geometric feature. This connection could be really useful in array design.

5. Case study

These curves can be used to establish constraints on the array geometry, when an array with certain *SLL* performance is required. Thanks to these constraints, the number of arrays to be evaluated

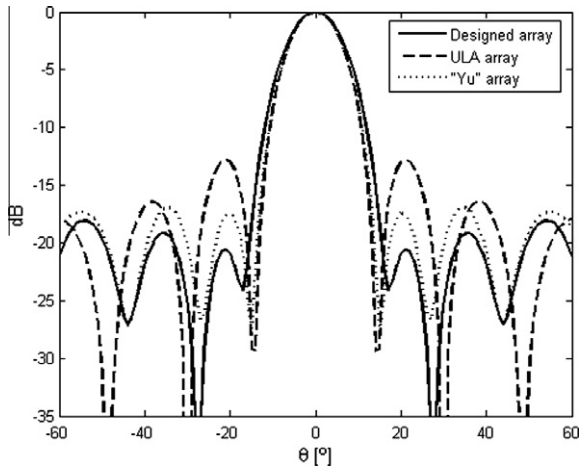


Fig. 3. Beampattern of the designed array.

can be reduced, and therefore the computational burden associated to the design technique as well.

This section shows an example of an array design algorithm that is based on a massive search over all those microphone arrays with eight sensors, a 3.5λ spatial aperture and a 0.28λ minimum sensor spacing ($\frac{1}{2}$ in. for a 7.5 kHz frequency, typical values for microphone size and work frequency). All these arrays have been generated varying element positions with 1 mm steps, i.e. a manually feasible variation of an element position, and fulfilling some geometric constraints based on the relationships defined in this work.

The purpose of this search is finding the best microphone array with a SLL_1 value better than -18 dB and improving SLL_{max} as much as possible, in a $\pm 60^\circ$ spatial angle, and according to the experimental quality function: $Q = (SLL_1 - 18) + (SLL_{max} - 10.5)^2$ [12]. This quality function has been optimised to track groups of speakers close together. In these situations, low SLL_1 values are necessary to be able to differentiate each speaker more accurately.

The geometric values associated to $SLL_1 = -18$ dB, according to the maximum probability functions, are $\sigma_x = 0.172\lambda$ and $X_{max} = 0.765\lambda$, and the SLL_{max} value associated to these defined geometric features is -10.5 dB. According to the geometric constraints over the required array, its σ_x and X_{max} values must be included in the intervals centred in the geometric values associated to the defined SLL_1 value (-18 dB), in this case:

$$(0.172\lambda - \zeta_{\sigma}) \leq \sigma_{x,array} \leq (0.172\lambda + \zeta_{\sigma}) \text{ and } (0.765\lambda - \zeta_{X_{max}}) \leq X_{max,array} \leq (0.765\lambda + \zeta_{X_{max}}),$$

where ζ_{σ} and $\zeta_{X_{max}}$ are the interval widths for σ_x and X_{max} , respectively. These interval widths are defined as the 2% of the total width of the effective area for the corresponding geometric parameter.

From among the 2×10^8 valid arrays that have been generated, only 3.8×10^6 of them fulfil the geometric constraints. Thus, thanks to these constraints over the geometry, computational burden has been reduced by a 52.6 factor if this computational burden is considered to be proportional to the number of arrays to be evaluated.

Fig. 3 shows a comparison between the beampattern of the array that shows the best performance according to the defined quality function (solid line) and the beampattern of a ULA with eight sensors and an equivalent 3.5λ spatial aperture (dashed line). The SLL values of the designed array are $SLL_1 = -21.04$ dB and $SLL_{max} = -17.86$ dB, and the corresponding geometric features are $X_{max} = 0.77\lambda$ and $\sigma_x = 0.17\lambda$. The SLL values of the ULA are $SLL_1 = SLL_{max} = -13.23$ dB, and the corresponding geometric features are $X_{max} = 0.5\lambda$ and $\sigma_x = 0$. It can be observed that in the

angular excursion of interest, i.e. $\pm 60^\circ$, the designed array has better SLL_1 and SLL_{max} values. Furthermore, this designed array has the desired array characteristic, i.e. a low SLL_1 value. This characteristic allows a more accurate differentiation of speakers close together.

Fig. 3 also shows a comparison between the beampattern of this designed array and the beampattern of another optimised array, the one designed by Yu in [13] (dash dotted line). The SLL values of Yu's array are $SLL_1 = -17.38$ dB and $SLL_{max} = -16.93$ dB. Even though Yu's design focuses array quality on a maximum sidelobe level as low as possible, it can be observed that the designed array shows lower sidelobe levels although the designed array is made up of eight sensors and Yu's array has ten sensors.

6. Conclusions

The performance offered by acoustic array-based solutions is conditioned to the performance of the array itself. The search of an array design with the best performance is associated to a computational burden. Thus, reducing this computational burden means a significant improvement in the design technique and therefore of the cost of the implemented solution.

This paper exploits the statistical relationship between array geometry and performance. Specifically, this paper explains a methodology to obtain maximum probability functions that give a direct association, in a statistical sense, between different measures of sidelobe levels and the spacing of elements in random linear arrays with a small number of sensors. Sidelobe levels chosen for this analysis are first sidelobe level (SLL_1), maximum sidelobe level (SLL_{max}) and average sidelobe level (\overline{SLL}), and the corresponding array geometric parameters are standard deviation of sensor spacing (σ_x) and maximum spacing (X_{max}). One of the novelties of this work is the relationship among these three sidelobe level parameters in the same analysis.

From these functions, most probable limits of sidelobe level values for random linear arrays can be determined and also a sidelobe level interrelation can be established. With this interrelation, fixing a value of one of the considered sidelobe levels, the value of the sensor spacing parameters that are most probable to offer this fixed sidelobe level value can be obtained. And, through these spacing parameters, the most probable values associated to the other two sidelobe levels are established.

These relationships can be employed to pre-select those arrays more likely to offer some specific sidelobe level performance by analysing their sensor spacing parameters. In this way, computational burden can be reduced in an array design optimisation, avoiding the calculation of the beampattern for those arrays rejected during the pre-selection procedure. These geometry vs. performance relationships can also be employed to generate initial element distributions on optimisation algorithms, such as Genetic Algorithms and Simulated Annealing. In optimisation processes, a good selection of initial conditions is very important in order to guarantee stability and fast convergence.

References

- [1] Kitagawa T, Thompson DJ. The horizontal directivity of noise radiated by a rail and implications for the use of microphone arrays. *J Sound Vib* 2010;329:202–20.
- [2] Liu H, Milios E. Acoustic positioning using multiple microphone arrays. *J Acoust Soc Am* 2005;117(5):2772–82.
- [3] Li J, Akagi M. A hybrid microphone array post-filter in a diffuse noise field. *Appl Acoust* 2008;69:546–57.
- [4] Brandes TS, Benson RH. Sound source imaging of low-flying airborne targets with an acoustic camera array. *Appl Acoust* 2007;68:752–65.
- [5] Van Veen B, Buckley K. Beamforming: a versatile approach to spatial filtering. *IEEE ASP Mag* 1988;4–24.
- [6] Steinberg B. Comparison between the peak sidelobe of the random array and algorithmically designed aperiodic arrays. *IEEE Trans Anten Propag* 1973;21:366–9.

- [7] Unz H. Linear arrays with arbitrarily distributed elements. *IRE Trans . Anten Propag* 1960;8(2):222–3.
- [8] Kumar B, Branner G. Generalized analytical technique for the synthesis of unequally spaced arrays with linear planar cylindrical and spherical geometry. *IEEE Trans Anten Propag* 2005;53(2):621–34.
- [9] Fourikis N. *Advanced array systems. Applications and RF technologies*. London: Academic Press; 2000.
- [10] Lo YT. A Mathematical theory of antenna arrays with randomly spaced elements. *IEEE Trans Anten Propag* 1964;12(5):257–68.
- [11] L. del Val et al. Geometric properties of random arrays for beamforming. In: *IASTED international conference on signal and image processing*, Kailua-Kona, HI, USA; 18–20 August 2008.
- [12] L. del Val, *Optimisation of directional sensor positions based on geometric selection strategies for beamforming*. In: *Ph.D dissertation, Department of Signal Theory and Communications and Telematic Engineering, universidad de valladolid, Valladolid*; 2008.
- [13] Yu C-C. Sidelobe reduction of asymmetric linear array by spacing perturbation. *Electron Lett* 1997;33(9):730–2.